

Fully stable dS vacua from generalised fluxes

Johan Blåbäck, Ulf Danielsson and Giuseppe Dibitetto

Institutionen för fysik och astronomi,

Uppsala Universitet,

Box 803, SE-751 08 Uppsala, Sweden

{johan.blaback, ulf.danielsson, giuseppe.dibitetto}@physics.uu.se

ABSTRACT

We investigate the possible existence of (meta-)stable de Sitter vacua within $\mathcal{N} = 1$ compactifications with generalised fluxes. With the aid of an algorithm inspired by the method of differential evolution, we were able to find three novel examples of completely tachyon-free de Sitter extrema in a non-isotropic type IIB model with non-geometric fluxes. We also analyse the surroundings of the aforementioned points in parameter space and chart the corresponding stability regions. These happen to occur at small values of the cosmological constant compared to the AdS scale.

Introduction

The possible existence of (meta-)stable de Sitter (dS) vacua in string theory, is considered to be of crucial importance if we want to achieve agreement with the main cosmological observations of the last two decades. The problem has been addressed following various approaches using string compactifications, and their link with the corresponding effective descriptions. Focusing on particular effective supergravity descriptions, which often are referred to as *STU*-models, the introduction of fluxes turns out to be the key, at least perturbatively, for inducing a superpotential of the right form [1].

Within these supergravity models, several theories have been studied that describe string backgrounds in type IIA [2–13], and type IIB [14–19]. So far, there are no known example of a fully meta stable dS vacuum. All geometric compactifications have unstable directions already within the isotropic truncation of the *STU*-model. Using non-geometric fluxes [20] it was possible to construct the first example of an isotropically stable dS extremum [18]. This solution is still, however, unstable in the non-isotropic directions. This situation was recently analysed in a more systematic way in ref. [21].

The main result of this paper are the first examples of fully stable dS vacua in the *STU*-model. We show that non-geometric fluxes provide enough freedom in parameter space for tuning the masses of all the moduli to be positive, even the non-isotropic ones. In appendix A, we analyse the whole region of stable dS in parameter space around such stable dS points by providing some insightful plots. In appendix B, we give some details concerning the algorithm that allowed us to find the aforementioned stable dS vacua.

The $\mathbb{Z}_2 \times \mathbb{Z}_2$ orbifold with generalised fluxes

Orbifold compactifications of type IIB string theory on $T^6/(\mathbb{Z}_2 \times \mathbb{Z}_2)$ with O3/O7-planes (and duals thereof) with generalised fluxes can all be placed within the same framework of effective four-dimensional supergravity descriptions that are known as *STU*-models. These theories enjoy $\mathcal{N} = 1$ supersymmetry and $\text{SL}(2)^7$ global bosonic symmetry. The action of such a global symmetry on the fields and couplings can be interpreted as the effect of string dualities.

The scalar sector contains seven complex fields spanning the coset space $(\text{SL}(2)/\text{SO}(2))^7$ which we denote by $\Phi^\alpha \equiv (S, T_i, U_i)$ with $i = 1, 2, 3$. The kinetic Lagrangian follows from the Kähler potential

$$K = -\log(-i(S - \bar{S})) - \sum_{i=1}^3 \log(-i(T_i - \bar{T}_i)) - \sum_{i=1}^3 \log(-i(U_i - \bar{U}_i)) . \quad (1)$$

This yields

$$\mathcal{L}_{\text{kin}} = \frac{\partial S \partial \bar{S}}{(-i(S - \bar{S}))^2} + \sum_{i=1}^3 \left(\frac{\partial T_i \partial \bar{T}_i}{(-i(T_i - \bar{T}_i))^2} + \frac{\partial U_i \partial \bar{U}_i}{(-i(U_i - \bar{U}_i))^2} \right). \quad (2)$$

The presence of fluxes induces a scalar potential V for the moduli fields which is given in terms of the above Kähler potential and a holomorphic superpotential W by

$$V = e^K \left(-3 |W|^2 + K^{\alpha\bar{\beta}} D_\alpha W D_{\bar{\beta}} \bar{W} \right), \quad (3)$$

where $K^{\alpha\bar{\beta}}$ is the inverse Kähler metric and D_α denotes the Kähler-covariant derivative.¹

The general form of a superpotential induced by locally geometric fluxes in type IIB with O3/O7-planes is given by

$$W = \underbrace{P_F(U_i)}_{F \text{ flux}} + S \underbrace{P_H(U_i)}_{H \text{ flux}} + \sum_k T_k \underbrace{P_Q^{(k)}(U_i)}_{Q \text{ flux}} + S \sum_k T_k \underbrace{P_P^{(k)}(U_i)}_{P \text{ flux}}, \quad (4)$$

where P_F , P_H , $P_Q^{(k)}$ and $P_P^{(k)}$ are cubic polynomials in the complex structure moduli given by

$$\begin{aligned} P_F(U_i) &= a_0 - \sum_i a_1^{(i)} U_i + \sum_i a_2^{(i)} \frac{U_1 U_2 U_3}{U_i} - a_3 U_1 U_2 U_3, \\ P_H(U_i) &= -b_0 + \sum_i b_1^{(i)} U_i - \sum_i b_2^{(i)} \frac{U_1 U_2 U_3}{U_i} + b_3 U_1 U_2 U_3, \\ P_Q^{(k)}(U_i) &= c_0^{(k)} + \sum_i c_1^{(ik)} U_i - \sum_i c_2^{(ik)} \frac{U_1 U_2 U_3}{U_i} - c_3^{(k)} U_1 U_2 U_3, \\ P_P^{(k)}(U_i) &= -d_0^{(k)} - \sum_i d_1^{(ik)} U_i + \sum_i d_2^{(ik)} \frac{U_1 U_2 U_3}{U_i} + d_3^{(k)} U_1 U_2 U_3. \end{aligned} \quad (5)$$

The IIA and IIB interpretation of the above superpotential couplings is summarised in table 1. Note that by having the possibility of choosing T-duality frame, observables that are not invariant under T-duality will differ depending on what frame is chosen.

Fully stable de Sitter vacua

The setup we focus on is the IIB duality frame with O3- and O7-planes with generalised fluxes defining a locally geometric background, *i.e.* F_3 , H , Q and P fluxes. In ref. [21] it was recently argued that, whenever one includes a number of fluxes equal to twice the number N of real fields in the theory, there is just enough freedom for casting the equations of motion into the form of a set of linear conditions, when the scalars are taken at the origin Φ_0 of moduli space. The space of solutions of the full problem will then have dimension N . The

¹We are working in units where $M_{\text{Pl}} = 1$.

couplings	Type IIB	Type IIA	fluxes	dof's
1	F_{mnp}	F_{ambncp}	a_0	1
U_i	F_{mnc}	F_{ambn}	$-a_1^{(i)}$	3
$U_j U_k$	F_{mbc}	F_{am}	$a_2^{(i)}$	3
$U_i U_j U_k$	F_{abc}	F_0	$-a_3$	1
S	H_{mnp}	H_{mnp}	$-b_0$	1
$S U_i$	H_{mnc}	$\omega_{mn}{}^c$	$b_1^{(i)}$	3
$S U_j U_k$	H_{mbc}	$Q_m{}^{bc}$	$-b_2^{(i)}$	3
$S U_i U_j U_k$	H_{abc}	R^{abc}	b_3	1
T_i	$Q_p{}^{ab}$	H_{abp}	$c_0^{(i)}$	3
$T_i U_j$	$Q_p{}^{an} = Q_p{}^{mb} , Q_a{}^{bc}$	$\omega_{pa}{}^n = \omega_{bp}{}^m , \omega_{bc}{}^a$	$c_1^{(ji)}$	9
$T_l U_i U_j$	$Q_c{}^{mb} = Q_c{}^{an} , Q_p{}^{mn}$	$Q_b{}^{cm} = Q_a{}^{nc} , Q_p{}^{mn}$	$-c_2^{(kl)}$	9
$T_l U_i U_j U_k$	$Q_c{}^{mn}$	R^{mnc}	$-c_3^{(l)}$	3
$S T_i$	$P_p{}^{ab}$		$-d_0^{(i)}$	3
$S T_i U_j$	$P_p{}^{an} = P_p{}^{mb} , P_a{}^{bc}$		$-d_1^{(ji)}$	9
$S T_l U_i U_j$	$P_c{}^{mb} = P_c{}^{an} , P_p{}^{mn}$		$d_2^{(kl)}$	9
$S T_l U_i U_j U_k$	$P_c{}^{mn}$		$d_3^{(l)}$	3

Table 1: Mapping between fluxes and couplings in the superpotential both in type IIB with O3 and O7 and in type IIA with O6. The six internal directions of T^6 are split into “ $-$ ” labelled by $m = 1, 3, 5$ and “ $|$ ” labelled by $a = 2, 4, 6$. Note that the empty boxes in type IIA are related to the presence of dual fluxes which do not even admit any local description. Note that the orbifold involution forces i, j, k to be all different any time they appear as indices of fields of the same type (T or U).

general solution will give the fluxes as a function of the N supersymmetry- (SUSY-)breaking parameters.

The SUSY-breaking parameters are N real constants A_α and B_α defined through

$$D_\alpha W|_{\Phi_0} = A_\alpha + iB_\alpha . \quad (6)$$

In our non-isotropic locally geometric setup with $N = 14$ real fields, one would then need to consider 28 fluxes in order to apply the prescription of ref. [21] to the search for stable dS vacua. The set of 28 superpotential couplings that we have chosen here corresponds to

the most general F_3 and H fluxes plus the first half of Q flux components in type IIB. From table 1, this set reads

$$\left\{ a_0, a_1^{(i)}, a_2^{(i)}, a_3, b_0, b_1^{(i)}, b_2^{(i)}, b_3, c_0^{(i)}, c_1^{(ij)} \right\} . \quad (7)$$

The goal of this paper is to perform a scan of the 14-dimensional parameter space of solutions searching for fully stable dS extrema. In ref. [21] it was already argued that a random scan would not be efficient enough for finding special tachyon-free dS extrema, since the fraction of such points in the dS region is expected to be extremely tiny.

To overcome this difficulty, we have designed an evolutionary algorithm, which has the property of flowing in parameter space towards better-behaved solutions, *i.e.* positive cosmological constant and positive eigenvalues of the mass matrix. This algorithm is presented in detail in appendix B.

Letting the algorithm run with the input parameters given in appendix B gave rise to 3 fully stable dS vacua, which are shown in table 2. The full set of flux numbers for these solutions are specified in table 3 in appendix A .

	Sol. 1		Sol. 2		Sol. 3	
$V_0 \equiv V(\Phi_0)$	8.85×10^{-6}		1.58×10^{-5}		1.00×10^{-4}	
$\tilde{\gamma} \equiv \frac{ DW ^2}{3 W ^2}$	1.00008		1.00012		1.00065	
Normalised masses (m^2/V_0)	1.85148×10^6	1.78128×10^6	262778	259704	34702.4	28731.5
	1.31064×10^6	1.27212×10^6	160140	153601	25215.5	18728.6
	113890	94187.9	24219.8	11296.3	5370.90	3609.62
	23907.3	11397.5	9273.53	7282.96	1572.22	1179.86
	5290.32	1478.37	4155.21	1745.39	723.060	518.923
	1353.35	607.799	1306.57	343.391	188.606	145.959
	17.9045	2.85612×10^{-3}	24.7202	11.4504	5.16471	9.52228×10^{-4}

Table 2: *The physical quantities characterising the 3 stable dS extrema found through the algorithm presented in appendix B. The first row shows the values of the cosmological constant, the second row the normalised energy $\tilde{\gamma}$, and finally the third row shows the full mass spectra normalised to the cosmological constant.*

Finally we would like to carry out a complementary analysis w.r.t. the search that we have just presented. The aim is to map out the region of stable dS inside parameter space in the IIB case previously introduced and studied. By means of such an analysis one can study how stable dS vacua organise themselves in the parameter space spanned by $\{A_\alpha, B_\alpha\}$.

For each of the 3 stable dS extrema, we have plotted the level curves of $\tilde{\gamma} \equiv \frac{|DW|^2}{3|W|^2}$ and of $\eta \equiv \text{Min} \left\{ \text{Eigenvalues} \left((m^2)^I_J \right) \right\}$ in the (A_S, B_S) plane. Subsequently we found the regions where $\tilde{\gamma} > 1$ and $\eta > 0$, corresponding to stable dS critical points. These results are depicted in figure 1 for the three solutions.

Our present understanding of the plots suggests that stable dS vacua organise themselves into thin sheets in parameter space. This conclusion seems to be perfectly in line with what was found in ref. [21] in the isotropic case where only $N = 6$ real fields were retained in the model.

Conclusions

We have in this work presented three de Sitter vacua which are stable in all of the $N = 14$ considered non-isotropic directions. These de Sitter vacua were obtained using the framework of the *STU*-models, more specifically $\mathbb{Z}_2 \times \mathbb{Z}_2$ orbifold compactifications with generalised fluxes. We used a setup containing $N = 14$ real fields, with $N = 14$ supersymmetry-breaking parameters and $2N = 28$ fluxes; F_3 , H and non-geometric flux Q . This result shows that the addition of non-geometric flux provides enough freedom to allow for stable de Sitter solutions.

The details of the de Sitter solutions, the size of the cosmological constant and the values of the masses can be found in table 2. Eventough all masses are non-tachyonic there are two cases where the masses are very small compared to the value of the potential – which might indicate the possibility of an instability. However this is not a general feature of these solutions, since only two out of three solutions contain such low masses. We have also included table 3 for the reader interested in the details of the values of the fluxes. These solutions were obtained via an evolutionary algorithm designed to seek out stable de Sitter regions. We have included a description of our implementation of this algorithm in appendix B.

As expected by ref. [21], these solutions are part of stable de Sitter regions that are organised into sheets or small regions - an overlap between regions with positive cosmological constant and stability - as can be seen in 2-dimensional slices of the $N = 14$ dimensional parameter space. We have included plots of these regions in the vicinity of the found stable de Sitter solutions in figure 1. The structure and occurrence of these overlapping regions is very fascinating and is something we plan to investigate further in the future.

Another very interesting question is whether the supergravity approximation is valid when the non-geometric fluxes are added. Because of the absence of a full description of

the non-geometric fluxes in 10D it is hard to believe that it would be. However as a future investigation we plan to study the supergravity approximation in terms of 4D supergravity where non-geometric fluxes could be an acceptable addition.

Acknowledgments

We would like to thank Kristoffer Ekman Wärja for discussions regarding evolutionary algorithms. The work of the authors is supported by the Swedish Research Council (VR), and the Göran Gustafsson Foundation.

A Flux values and figures

	Sol. 1	Sol. 2	Sol. 3
$A_S \quad B_S$	-0.314252 -0.677296	0.266259 0.0513389	-0.586674 -0.186345
$A_{T_1} \quad B_{T_1}$	-0.145819 0.201488	0.0113161 1.19326	0.684213 0.846619
$A_{T_2} \quad B_{T_2}$	0.324296 0.200242	-0.374583 -0.318198	0.540869 1.10608
$A_{T_3} \quad B_{T_3}$	-0.510199 -0.830019	0.0745176 0.814969	-0.373167 0.724434
$A_{U_1} \quad B_{U_1}$	0.437796 -0.223916	-0.410472 0.56115	-0.265422 0.187632
$A_{U_2} \quad B_{U_2}$	-0.10521 -0.716205	-0.074538 0.276484	-0.118099 0.651658
$A_{U_3} \quad B_{U_3}$	-0.110376 -0.952221	-0.597945 0.903104	-0.297359 0.75668
$a_0 \quad b_0$	0.249727 1.26278	-0.0809612 -0.470688	-0.126241 0.505546
$a_1^{(i)} \quad b_1^{(i)}$	-0.385558 -1.00688	0.763615 0.637699	0.0845892 -0.342897
	3.24742 3.23091	-0.129007 -1.32755	-0.00376873 0.431055
	-3.42277 -1.65416	-0.258342 -0.502742	-0.687791 -1.81103
$a_2^{(i)} \quad b_2^{(i)}$	-0.678952 0.269654	-1.69969 -0.585701	-0.748501 -0.346495
	4.77196 -2.82032	0.141055 -0.0290134	2.79635 -0.40546
	-4.74382 3.85504	2.04863 0.623729	-2.13249 0.457822
$a_3 \quad b_3$	-0.626634 0.244097	-0.0281293 -0.0877685	-0.446200 -0.270327
$c_0^{(i)}$	0.210031	0.224759	0.471208
	0.680146	-0.16114	0.327864
	-0.154349	0.287961	-0.586172
$c_1^{(ij)}$	0.934579 0.932678 0.134729	1.00141 -1.58335 -2.92823	-0.108522 0.144519 -1.70585
	1.3931 0.978188 0.351523	-0.335711 -0.460028 0.806899	0.178853 -0.083869 1.47008
	-1.12313 -0.707561 -0.313208	-0.628606 0.56901 1.78014	-0.489907 -0.220766 -0.305991

Table 3: *The 3 stable dS extrema found through the algorithm presented in appendix B. The first part of the table shows the values of the 14 SUSY-breaking parameters, whereas in the second part we give the explicit values of the 28 fluxes turned on at the corresponding critical points.*

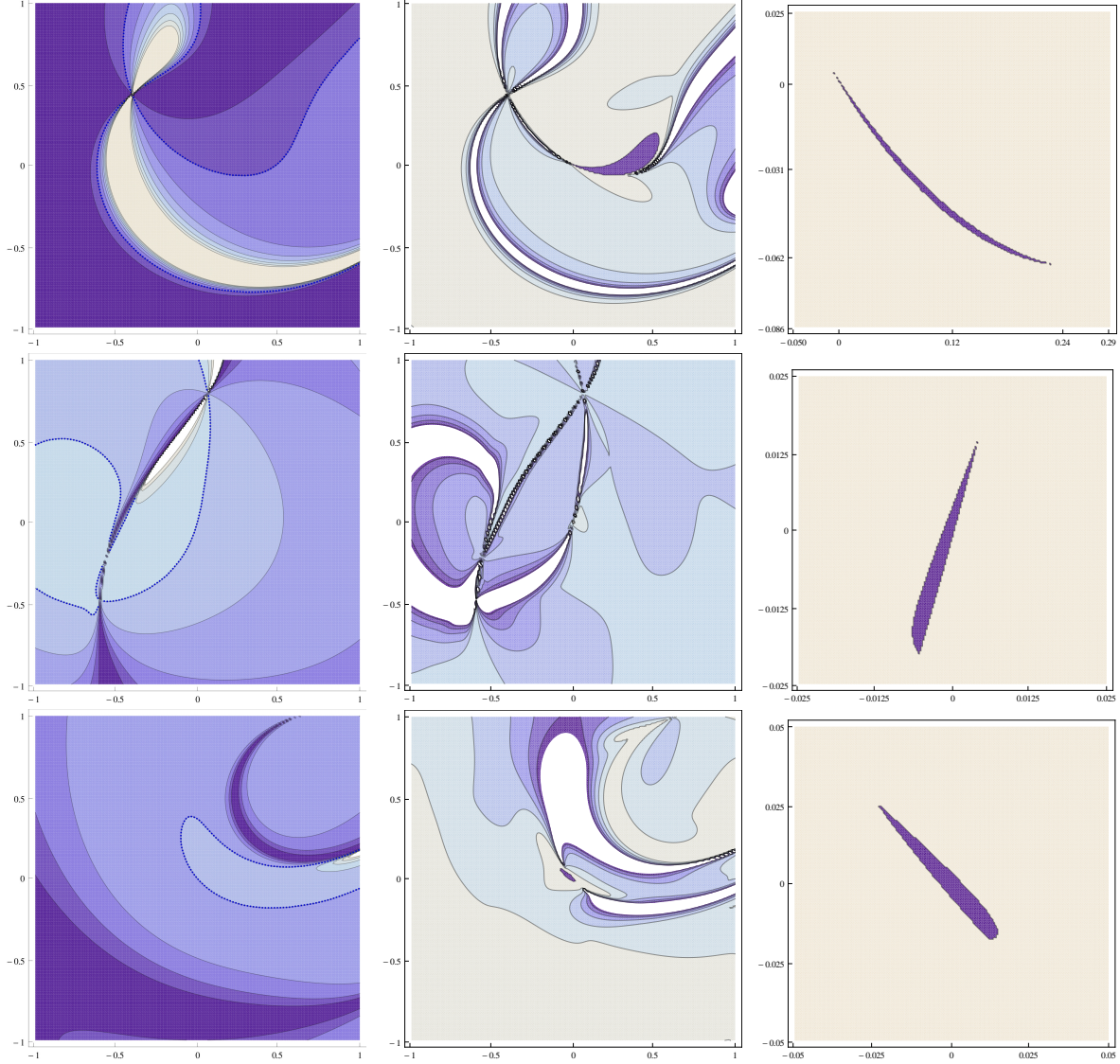


Figure 1: *The parameter space of solutions around Sol. 1, 2 and 3 (top, center and bottom), projected on the (A_S, B_S) plane. The origin in each picture is the found stable dS. Left: Level curves of the cosmological constant; the dS regions are the ones filled with lighter colours next to the Minkowski (blue dashed) lines. Middle: Level curves of the η parameter; the tachyon-free regions are filled with darker colours. Right: The tiny region of overlap in parameter space corresponding with stable dS is zoomed in here.*

B The algorithm

The search algorithm used is inspired by the methods of *differential evolution*. These are evolutionary algorithms that can walk in a solution landscape to find extremal points or special regions. Here we will describe the how the algorithm works and parts of the workings

of its implementation. We will start by presenting the steps of the algorithm, then proceed to explain them in closer detail.

The algorithm proceeds according to the following repeated scheme.

1. Generate a population (set of parents).
2. Create a mutated copy of the population (set of children).
3. Generate $\tilde{\gamma}$ and the mass eigenvalues for parents and children.
4. For each parent and child pair, choose the *better* one.
5. Check additional criteria and repeat until termination conditions.

Step 1. The system is determined when the 14 SUSY-breaking parameters are specified. The population is a set where each element contain values for each of the 14 SUSY-breaking parameters. This set can either be generated randomly, or by a particular choice. We chose to leave one parameter to be fixed by demanding that we start at a Minkowski point. The size of the population is a weigh-off against the amount of iterations one wants to get to in a certain time. A large population gives a higher chance of a better initial position in the parameter space, but more iterations would more likely converge into a de Sitter region.

Step 2. Performing a mutation is to take a step in some direction. This direction is random and so is the step size. This gives the algorithm the possibility to search freely without us imposing any explicit directions or step sizes. However, the randomness of the mutation should be chosen carefully - a mutation too random will make the algorithm a random-walk instead of being evolutionarily progressed. This is why the following code was chosen to mutate a member of the population

```
mutate[member0_, sigma0_] := Module[{member=member0, sigma=sigma0},
  Do[
    If[Not[RandomInteger[{1, 3}] == 1],
      member[[i]] = member[[i]] + RandomVariate[NormalDistribution[0, sigma]]
    ];
    ,{i, Length[member]}}];
  member
];
```

The step direction is random in the sense that there is a two in three chance that a number will be mutated. The size of the step is also random according to a normal distribution with zero mean. The standard deviation is given as input to this module, so that the algorithm can for example increase the effective step size if the solution gets stuck. There are hence two parameters we need to give to the algorithm that will affect its efficiency, *i.e.* the chance of getting mutated, and standard deviation for the mutation.

Step 3. For each member we need the $\tilde{\gamma}$ and the mass matrix, to later be able to compare solutions. A module is needed to solve the set of equations and produce these parameters.

This is where most of the computational time is spent; given the SUSY-breaking parameters one needs to solve N linear equations and compute the eigenvalues of a $N \times N$ matrix. This means that it is preferable to associate the $\tilde{\gamma}$ and each mass with every member of the population, to avoid calculating these more than once.

Step 4. Some function must be invented to decide whether the parent or child is the better solution. The choice made here was to have the following three criteria

1. Approaching range $\mathcal{N}(N^1, \sigma)$,
2. Getting within range $\mathcal{N}(N^2, \sigma)$,
3. Getting within numerically safe range $\mathcal{N}(N^3, \sigma)$,

where $\mathcal{N}(\mu, \sigma)$ denotes a random number chosen according to the normal distribution around the mean μ with standard deviation σ . This applies to each of the 15 parameters that specify a stable dS extremum when all within range, *i.e.* $\tilde{\gamma}$ plus the eigenvalues of the mass matrix. All of the above conditions receive a number, its magnitude depending on how desirable the condition is. The total value parametrising the solution's desirability is given by the algebraic sum of the 15 separate contributions. This parameter will judge whether or not the parent should be replaced by its mutated child. If one of the above criteria is exclusively not satisfied, it receives the corresponding negative number instead. In choosing this evaluation criterion, some limit cases should be considered - what to do in the case of one parameter approaching range and one getting further away, etc.. Our choice of the normal distribution with mean N^p , where the power p categorises the conditions by desirability is to make random choices in such conflicting cases. This is hence another parameter we need to give as input to the algorithm.

Step 5. There are also additional conditions that could be checked for the code being able to progress smoothly for an indefinite time or until max iterations. Such a condition could be how long a certain solution have been iterated without finding a better child. If the solution has stayed in the same position for too long, one might want to increase the size of the mutation (the standard deviation), to jump out of this position where it seemed not able to find stable de Sitter. This gives two parameters to input into the algorithm: how long before a solution is categorized as stuck and how much the standard deviation should increase. One could also imagine that if the solution is very close of having $\tilde{\gamma} > 1$ and all non-negative masses, that one would decrease the size of the mutation to zoom in on a smaller search area, however this was not implemented by us.

An additional check is to keep track of how long after a solution got stuck this should be removed and replaced. Since the search area is increasing after getting stuck, the chance of finding a better solution within reasonable time decreases. These solutions can be saved but

removed from the population, to be able to study them later if that is desired and to ensure the progression of the population. This gives another parameter as input to the algorithm. Similarly one should remove any stable de Sitter found, from the population and save it, this to make the population continue with the possibility to find more stable de Sitters.

A termination condition should be given for the loop. The number of iterations, together with the populations size, is a comfortable way to determine the time for the code to run.

As mentioned before, the algorithm has a number of parameters that needs to be specified. What follows are the values for these numbers which successfully produced stable de Sitter solutions.

Population size	16
Standard deviation for mutation	$\sigma_m = 0.01$
Chance to mutate a number	two in three
Condition desirability	$\mathcal{N}(N^p, \sigma)$ ($\sigma = 1$)
Iterations	50 000
Iterations without change until stuck	500
Growth of mutation standard deviation per iteration after stuck	$.5\sigma_m$
Iterations without change until removed from population	2000

References

- [1] S. B. Giddings, S. Kachru, and J. Polchinski, “Hierarchies from fluxes in string compactifications,” *Phys.Rev.* **D66** (2002) 106006, [arXiv:hep-th/0105097](#) [[hep-th](#)].
- [2] S. Kachru, M. B. Schulz, and S. Trivedi, “Moduli stabilization from fluxes in a simple IIB orientifold,” *JHEP* **0310** (2003) 007, [arXiv:hep-th/0201028](#) [[hep-th](#)].
- [3] J.-P. Derendinger, C. Kounnas, P. M. Petropoulos, and F. Zwirner, “Superpotentials in IIA compactifications with general fluxes,” *Nucl.Phys.* **B715** (2005) 211–233, [arXiv:hep-th/0411276](#) [[hep-th](#)].
- [4] O. DeWolfe, A. Giryavets, S. Kachru, and W. Taylor, “Enumerating flux vacua with enhanced symmetries,” *JHEP* **0502** (2005) 037, [arXiv:hep-th/0411061](#) [[hep-th](#)].
- [5] G. Villadoro and F. Zwirner, “N=1 effective potential from dual type-IIA D6/O6 orientifolds with general fluxes,” *JHEP* **0506** (2005) 047, [arXiv:hep-th/0503169](#) [[hep-th](#)].
- [6] J.-P. Derendinger, C. Kounnas, P. Petropoulos, and F. Zwirner, “Fluxes and gaugings: N=1 effective superpotentials,” *Fortsch.Phys.* **53** (2005) 926–935, [arXiv:hep-th/0503229](#) [[hep-th](#)].

- [7] O. DeWolfe, A. Giryavets, S. Kachru, and W. Taylor, “Type IIA moduli stabilization,” *JHEP* **0507** (2005) 066, [arXiv:hep-th/0505160](#) [[hep-th](#)].
- [8] R. Flauger, S. Paban, D. Robbins, and T. Wrase, “Searching for slow-roll moduli inflation in massive type IIA supergravity with metric fluxes,” *Phys.Rev.* **D79** (2009) 086011, [arXiv:0812.3886](#) [[hep-th](#)].
- [9] C. Caviezel, P. Koerber, S. Kors, D. Lust, T. Wrase, *et al.*, “On the Cosmology of Type IIA Compactifications on SU(3)-structure Manifolds,” *JHEP* **0904** (2009) 010, [arXiv:0812.3551](#) [[hep-th](#)].
- [10] U. H. Danielsson, S. S. Haque, G. Shiu, and T. Van Riet, “Towards Classical de Sitter Solutions in String Theory,” *JHEP* **0909** (2009) 114, [arXiv:0907.2041](#) [[hep-th](#)].
- [11] U. H. Danielsson, P. Koerber, and T. Van Riet, “Universal de Sitter solutions at tree-level,” *JHEP* **1005** (2010) 090, [arXiv:1003.3590](#) [[hep-th](#)].
- [12] U. H. Danielsson, S. S. Haque, P. Koerber, G. Shiu, T. Van Riet, *et al.*, “De Sitter hunting in a classical landscape,” *Fortsch.Phys.* **59** (2011) 897–933, [arXiv:1103.4858](#) [[hep-th](#)].
- [13] U. H. Danielsson, G. Shiu, T. Van Riet, and T. Wrase, “A note on obstinate tachyons in classical dS solutions,” [arXiv:1212.5178](#) [[hep-th](#)].
- [14] P. G. Camara, A. Font, and L. Ibanez, “Fluxes, moduli fixing and MSSM-like vacua in a simple IIA orientifold,” *JHEP* **0509** (2005) 013, [arXiv:hep-th/0506066](#) [[hep-th](#)].
- [15] G. Aldazabal, P. G. Camara, A. Font, and L. Ibanez, “More dual fluxes and moduli fixing,” *JHEP* **0605** (2006) 070, [arXiv:hep-th/0602089](#) [[hep-th](#)].
- [16] G. Aldazabal and A. Font, “A Second look at N=1 supersymmetric AdS(4) vacua of type IIA supergravity,” *JHEP* **0802** (2008) 086, [arXiv:0712.1021](#) [[hep-th](#)].
- [17] A. Guarino and G. J. Weatherill, “Non-geometric flux vacua, S-duality and algebraic geometry,” *JHEP* **0902** (2009) 042, [arXiv:0811.2190](#) [[hep-th](#)].
- [18] B. de Carlos, A. Guarino, and J. M. Moreno, “Flux moduli stabilisation, Supergravity algebras and no-go theorems,” *JHEP* **1001** (2010) 012, [arXiv:0907.5580](#) [[hep-th](#)].
- [19] B. de Carlos, A. Guarino, and J. M. Moreno, “Complete classification of Minkowski vacua in generalised flux models,” *JHEP* **1002** (2010) 076, [arXiv:0911.2876](#) [[hep-th](#)].
- [20] J. Shelton, W. Taylor, and B. Wecht, “Nongeometric flux compactifications,” *JHEP* **0510** (2005) 085, [arXiv:hep-th/0508133](#) [[hep-th](#)].
- [21] U. Danielsson and G. Dibitetto, “On the distribution of stable de Sitter vacua,” [arXiv:1212.4984](#) [[hep-th](#)].